THE JOURNAL OF BIOLOGICAL CHEMISTRY
Vol. 280, No. 35, Issue of September 2, pp. 31294–31302, 2005
Printed in U.S.A.

Interplay of Ca^{2+} and cAMP Signaling in the Insulin-secreting MIN6 β-Cell Line*[S]

Received for publication, May 24, 2005, and in revised form, June 24, 2005
Published, JBC Papers in Press, June 29, 2005, DOI 10.1074/jbc.M505657200

Luis R. Landa, Jr.‡§, Mark Harbeck‡§, Kelly Kaihara‡, Oleg Chepurny¶, Kajorn Kitiphongspattana‡, Oliver Graf‡, Viacheslav O. Nikolaev‖, Martin J. Lohse‖, George G. Holz¶, and Michael W. Roe‡

From the ‡Department of Medicine, The University of Chicago, Chicago, Illinois 60637, the ¶Department of Physiology and Neuroscience, New York University School of Medicine, New York, New York 10016, and the ‖Institute of Pharmacology and Toxicology, University of Würzburg, D-97078 Würzburg, Germany

Ca^{2+} and cAMP are important second messengers that regulate multiple cellular processes. Although previous studies have suggested direct interactions between Ca^{2+} and cAMP signaling pathways, the underlying mechanisms remain unresolved. In particular, direct evidence for Ca^{2+}-regulated cAMP production in living cells is incomplete. Genetically encoded fluorescence resonance energy transfer-based biosensors have made possible real-time imaging of spatial and temporal gradients of intracellular cAMP concentration in single living cells. Here, we used confocal microscopy, fluorescence resonance energy transfer, and insulin-secreting MIN6 cells expressing Epac1-camps, a biosynthetic unimolecular cAMP indicator, to better understand the role of intracellular Ca^{2+} in cAMP production. We report that depolarization with high external K^+, tolbutamide, or glucose caused a rapid increase in cAMP that was dependent on extracellular Ca^{2+} and inhibited by nitrendipine, a Ca^{2+} channel blocker, or 2′,5′-dideoxyadenosine, a P-site antagonist of transmembrane adenylate cyclases. Stimulation of MIN6 cells with glucose in the presence of tetraethylammonium chloride generated concomitant Ca^{2+} and cAMP oscillations that were abolished in the absence of extracellular Ca^{2+} and blocked by 2′,5′-dideoxyadenosine or 3-isobutyl-1-methylxanthine, an inhibitor of phosphodiesterase. Simultaneous measurements of Ca^{2+} and cAMP concentrations with Fura-2 and Epac1-camps, respectively, revealed a close temporal and causal interrelationship between the increases in cytoplasmic Ca^{2+} and cAMP levels following membrane depolarization. These findings indicate highly coordinated interplay between Ca^{2+} and cAMP signaling in electrically excitable endocrine cells and suggest that Ca^{2+}-dependent cAMP oscillations are derived from an increase in adenylate cyclase activity and periodic activation and inactivation of cAMP-hydrolyzing phosphodiesterase.

Ca^{2+} and cAMP are ubiquitous second messengers that regulate many cellular functions, including gene expression, protein biosynthesis, and exocytosis. In eukaryote cells, Ca^{2+} and cAMP signaling cascades are interconnected and often exhibit subcellular concentration gradients that are spatially and temporally heterogeneous (1–4). Intracellular cAMP concentration can be affected by activation of Ca^{2+}-sensitive isoforms of adenylate cyclase (5–7) and phosphodiesterase (8, 9). Conversely, cAMP and protein kinase A modulation of Ca^{2+} channels and plasma membrane Ca^{2+}-ATPases influences Ca^{2+} signal transduction (4, 10–14). The way in which these dynamic signals are integrated in single cells remains unresolved.

Only two studies have reported measurements of both second messenger signaling pathways simultaneously in single cells (15, 16). Concurrent imaging of cAMP and Ca^{2+} in C6-2B glioma cells and REF-52 fibroblasts loaded with FlCRhR, a recombinant fluorescence resonance energy transfer (FRET)[1]-based cAMP indicator, and Fura-2 revealed that the increase in intracellular Ca^{2+} following application of thapsigargin and ionomycin causes a decrease in isoproterenol-stimulated cAMP accumulation in C6-2B glioma cells, but not in REF-52 fibroblasts (15). In *Rana esculenta* ventricular cells, simultaneous detection of cAMP with FlCRhR and whole cell L-type Ca^{2+} current by patch-clamp electrophysiology indicated that increases in cAMP production activate Ca^{2+} channel conductance (16).

Spontaneous Ca^{2+} and cAMP increases have been observed in embryonic *Xenopus* neurons loaded with Fluo-4, a fluorescent Ca^{2+} indicator, and FlCRhR (17). The cells generate three to four pulses of cAMP/h, each lasting 3–7 min. cAMP accumulation appears to affect Ca^{2+} spiking; the frequency of spontaneous Ca^{2+} transients (3–10/h) is increased by application of forskolin, an activator of adenylate cyclase (AC), and decreased by inhibition of protein kinase A with KT5720. Stimulation of neurons with pulses (12/min) of forskolin and 3-isobutyl-1-methylxanthine (IBMX) also increases Ca^{2+} spike frequency. On the other hand, elimination of the spontaneous Ca^{2+} transients inhibits cAMP production, whereas transient Ca^{2+} spikes evoked by pulses of 100 mM KCl generate cAMP transients in embryonic *Xenopus* neurons. Although these elegant studies suggested a role for AC and protein kinase A in mediating the cAMP-induced effects on Ca^{2+} signaling and confirmed that the formation of cAMP is Ca^{2+}-dependent, the temporal interrelationships were

* This work was supported by research grants from the American Diabetes Association (to G. G. H. and M. W. R.) and by National Institutes of Health Grant DK45817 (to G. G. H.) and Grants DK63493, DK64162, and DK68822 (to M. W. R.). The costs of publication of this article were defrayed in part by the payment of page charges. This article must therefore be hereby marked "*advertisement*" in accordance with 18 U.S.C. Section 1734 solely to indicate this fact.

[S] The on-line version of this article (available at http://www.jbc.org) contains supplemental Fig. S1 and Table 1.

§ Both authors contributed equally to this work.

** To whom correspondence should be addressed: Dept. of Medicine MC-1027, The University of Chicago, 5841 South Maryland Ave., Chicago, IL 60637. Tel.: 773-702-4965; Fax: 773-834-0486; E-mail: mroe@medicine.bsd.uchicago.edu.

[1] The abbreviations used are: FRET, fluorescence resonance energy transfer; AC, adenylate cyclase; IBMX, 3-isobutyl-1-methylxanthine; ECFP, enhanced cyan fluorescent protein; EYFP, enhanced yellow fluorescent protein; $[cAMP]_c$, cytoplasmic cAMP concentration; $[Ca^{2+}]_c$, cytoplasmic Ca^{2+} concentration; DDA, 2′,5′-dideoxyadenosine; PDE, phosphodiesterase; TEA, tetraethylammonium chloride.

not directly established in these experiments because the two signals were not measured simultaneously.

We sought to better understand the temporal and causal interrelationships between Ca^{2+} and cAMP signals by real-time imaging. To accomplish this, we developed a new methodology that allows simultaneous measurements of Ca^{2+} and cAMP in single cells. We show in insulin-secreting MIN6 β-cells expressing Epac1-camps, a biosynthetic FRET-based cAMP sensor (18), and loaded with the Ca^{2+} indicator Fura-2 (19) that cAMP and Ca^{2+} signals are tightly coupled. The data suggest that increased production of cAMP following stimulation with secretagogues is dependent on Ca^{2+} influx through L-type voltage-dependent Ca^{2+} channels. We also observed rapid and transient Ca^{2+}-induced cAMP oscillations. Our findings indicate that Ca^{2+} and cAMP signals interact as a coordinated network capable of producing diverse temporal signaling patterns in electrically excitable endocrine cells.

EXPERIMENTAL PROCEDURES

Cell Culture—MIN6 cells (passages 18–30) were grown in Dulbecco's modified Eagle's medium supplemented with 10% heat-inactivated fetal bovine serum, 1 mM L-glutamine, 100 units/ml penicillin, 10 μg/ml streptomycin, and 55 μM β-mercaptoethanol and maintained in a humidified incubator with 95% air and 5% CO_2 at 37 °C.

Transfections—One day before transfection, MIN6 cells (5×10^5 cells) were plated on uncoated and sterilized 25-mm circular glass coverslips in 6-well tissue culture plates and maintained in complete Dulbecco's modified Eagle's medium. Cells were transiently transfected with 1 μg of plasmid encoding Epac1-camps (18) using Lipofectamine 2000 (Invitrogen) following the manufacturer's instructions. Transfection efficiencies ranged between 5 and 20%.

FRET Measurements and Ca^{2+} Imaging—Imaging experiments were conducted 48–96 h after transfection. The growth medium was removed and replaced with Krebs-Ringer bicarbonate solution containing 119 mM NaCl, 4.7 mM KCl, 2.5 mM $CaCl_2$, 1 mM $MgCl_2$, 1 mM KH_2PO_4, 25 mM $NaHCO_3$ or 10 mM HEPES-NaOH (pH 7.40), and 2 mM glucose. Coverslips were placed into a heated microperifusion chamber mounted on the specimen stage of an inverted fluorescence microscope (Nikon TE-2000U) equipped with a CARV spinning disk confocal system (Atto Bioscience Inc.). Cells were constantly superfused with Krebs-Ringer bicarbonate solution (2–5 ml/min) at 37 °C. For imaging Epac1-camps FRET, cells were visualized with a Nikon Super Fluor ×40 oil immersion or Nikon Plan Apo ×60 oil immersion objective. The Epac1-camps excitation wavelength was 440 nm and was attenuated 50–90% using neutral density filters. Dual emission ratio imaging at 485 nm (FRET donor, enhanced cyan fluorescent protein (ECFP)) and 535 nm (FRET acceptor, enhanced yellow fluorescent protein (EYFP)) was accomplished using a computer-controlled high speed filter wheel (Lambda 10-2 optical filter changer, Sutter Instrument Co., Novato, CA); the time for changing emission filters was 60–80 ms. Images (50–250-ms exposure) were captured with a 16-bit Cascade 650 digital camera (Roper Instruments) at 10-s intervals. Epac1-camps FRET decreases with increasing cAMP concentration; an increase in the 485/535 nm FRET emission ratio is indicative of an increase in cytoplasmic cAMP concentration ($[cAMP]_c$) (18).

For simultaneous measurements of intracellular Ca^{2+} and cAMP levels, we used Fura-2 to detect cytoplasmic Ca^{2+} concentration ($[Ca^{2+}]_c$) (19). Spectral separation of Epac1-camps and Fura-2 excitation and emission permits simultaneous imaging of $[cAMP]_c$ and $[Ca^{2+}]_c$ in single cells. The combination of Fura-2 and the FRET-based Ca^{2+} biosensor D1ER, which consists of ECFP and citrine (a variant of EYFP), has been used by Tsien and co-workers (20) to simultaneously measure $[Ca^{2+}]_c$ and endoplasmic reticulum Ca^{2+} concentration in HeLa and MCF-7 cells. For concurrent $[cAMP]_c$ and $[Ca^{2+}]_c$ measurements, MIN6 cells transiently transfected with Epac1-camps were loaded with 500 nM Fura-2 acetoxymethyl ester (Molecular Probes, Inc.) for 15–20 min at 37 °C. A Nikon Super Fluor ×40 oil immersion objective was used for these studies. 340- and 380-nm excitation filters and a 530-nm emission filter were used for Fura-2 dual excitation ratio imaging. A 455-nm dichroic filter (Chroma Technology Corp.) was used for Epac1-camps and Fura-2. Loading cells with Fura-2 acetoxymethyl ester did not affect maximum Epac1-camps responses following application of 10 μM forskolin and 100 μM IBMX, and conversely, Fura-2 detection of Ca^{2+} was not affected by Epac1-camps. Imaging data acquisition and analysis were accomplished using MetaMorph/MetaFluor software (Universal Imaging Corp.) and OriginPro 7E (OriginLab Corp.). Emission intensities were background-subtracted. Data are expressed as the ratio of FRET donor and acceptor emission (485/535 nm ratio) and the Fura-2 340 and 380 nm excitation (340/380 nm ratio). In addition, data were normalized to the average base-line values of the 485/535 and 340/380 nm ratios (485/535 and 340/380 nm relative ratios, respectively) to facilitate comparisons between responses in different cells. Data summaries are expressed as means ± S.E.

PCR and Nucleotide Sequence Analysis—Total RNA from MIN6 cells was extracted using an RNeasy kit (Qiagen Inc.). The RNA quality and quantity were determined in an Ultrospec 3000 spectrophotometer (Amersham Biosciences, Cambridge, UK). First-strand cDNA was generated with a reverse transcription system kit (Promega Corp., Madison, WI) using oligo(dT) primers following the manufacturer's protocol. Specific cDNA sequences were amplified in GeneAmp PCR System 9700 (Applied Biosystems, Foster City, CA) using REDTaq ReadyMix PCR Reaction Mix (Sigma). Amplified PCR products were run on 1.2% agarose gel and further characterized by DNA sequencing and BLAST analysis against the GenBank™ Data Bank.

RESULTS

cAMP Biosensor Expression and Function in MIN6 Cells—We transfected MIN6 cells with Epac1-camps, a biosynthetic FRET-based sensor that contains a single cAMP-binding domain of human Epac1 (exchange protein directly activated by cAMP 1) fused between ECFP and EYFP (18). Fluorescence from individual cells was easily detected 24 h after transfection. The intensity of fluorescence emission from ECFP and EYFP was 2–8-fold higher than autofluorescence from untransfected cells. As in Chinese hamster ovary cells and mouse primary neurons and peritoneal macrophages (18), Epac1-camps was distributed throughout the cytoplasm and excluded from the nucleus in MIN6 cells (Fig. 1*A*).

The unimolecular biosynthetic cAMP indicators, including Epac1-camps, Epac2-camps, ICUE1, ICUE2, and cyan fluorescent protein-Epac-yellow fluorescent protein (18, 21, 22), rely on cAMP-dependent FRET between chromophores of two mutants of green fluorescent protein as the basis for optical measurements of intracellular cAMP gradients. The green fluorescent protein mutants in Epac1-camps are ECFP and EYFP. Binding of cAMP to Epac induces a conformational change in Epac1-camps that increases the distance between ECFP and EYFP. As $[cAMP]_c$ rises, FRET between ECFP and EYFP declines, causing fluorescence emission from ECFP to increase and from EYFP to decrease. The ratio of ECFP (FRET donor) and EYFP (FRET acceptor) fluorescence emission is indicative of $[cAMP]_c$. FRET between ECFP and EYFP in individual MIN6 cells was measured by spinning disk confocal microscopy. We observed heterogeneity of the FRET emission intensity ratio in unstimulated cells (Fig. 1*A*). This raises the possibility that the FRET ratio heterogeneity might reflect regional variation in $[cAMP]_c$ and suggests that MIN6 β-cell cAMP is regulated by different mechanisms in distinct subregions. More work will need to be done to explore these hypotheses.

We tested the function of the sensor by measuring responses to reagents that stimulate cAMP production. Approximately 60 s (n = 20 cells) after application of 10 nM exendin-4, a glucagon-like peptide-1 receptor agonist that increases cAMP, Epac1-camps FRET decreased (Fig. 1*B*), and the FRET donor/acceptor emission ratio increased (Fig. 1*C*). The FRET ratio increased to maximum levels that were ~20–30% greater than base-line values (Fig. 1*D*). A similar response was elicited by 10 μM forskolin, an activator of AC (Fig. 1*E*).

Effect of Secretagogues on cAMP Formation—We used Epac1-camps to determine the effect of secretagogues on $[cAMP]_c$. Depolarization with 20 mM KCl (Fig. 2*A*) or 100 μM tolbutamide (Fig. 2*B*) caused a monophasic increase in cAMP. Stimulation with 20 mM glucose also increased production of cAMP in MIN6 cells (Fig. 2*C*). We tested whether the secretagogue-induced cAMP formation was due to activation of AC by

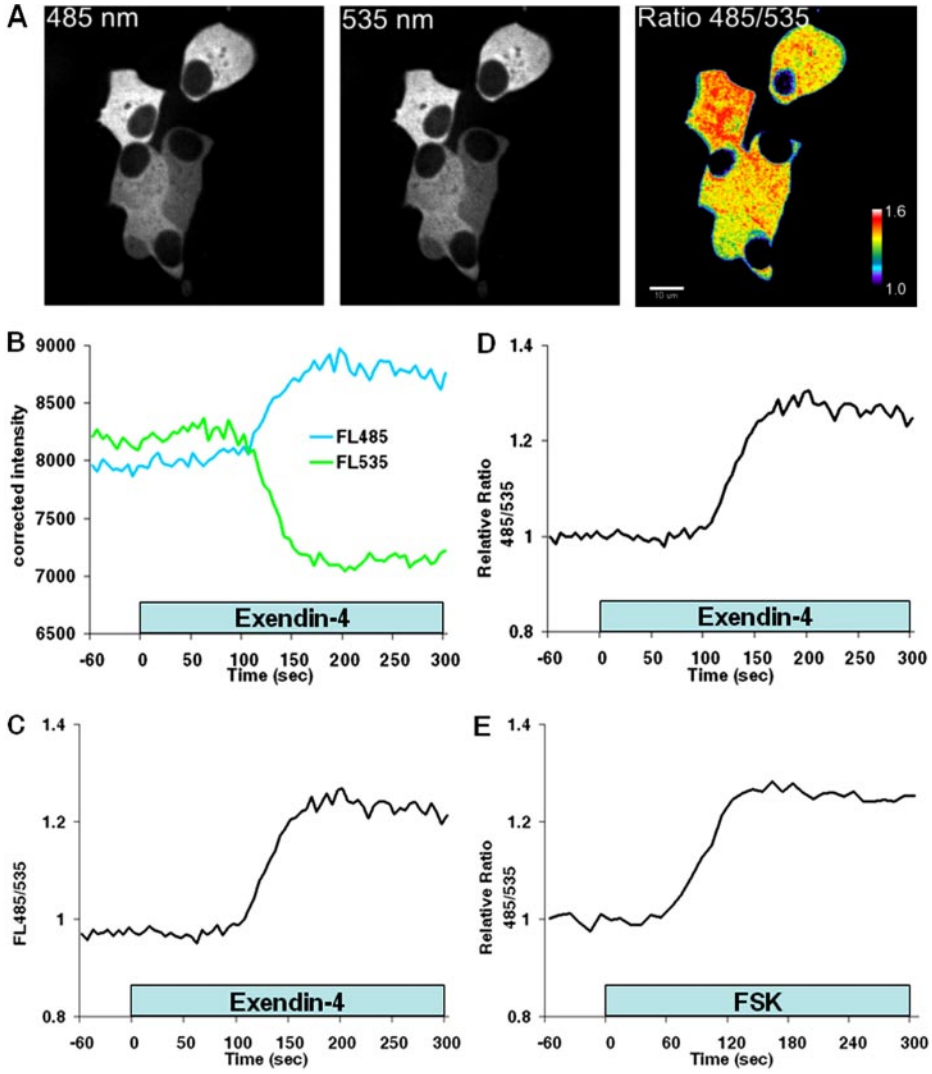

FIG. 1. **cAMP biosensor expression and function in MIN6 cells.** *A*, confocal images of MIN6 cells transiently expressing Epac1-camps. Distribution of the biosensor was cytoplasmic and excluded from the nucleus and other organelles. The pseudo-colored display of the FRET donor (*485 nm panel*) and acceptor (*535 nm panel*) emission intensity ratio (*Ratio 485/535 panel*) suggests regional variation in $[cAMP]_c$. The *color bar* depicts the range of 485/535 nm ratio values. *Scale bar* = 10 μm. *B–D*, kinetics of the Epac1-camps response in the same MIN6 cell. *B*, time-dependent change in Epac1-camps FRET donor (ECFP; *FL485*) and acceptor (EYFP; *FL535*) fluorescence after application of 10 nM exendin-4. *Traces* illustrate the average fluorescence intensity of Epac1-camps FRET recorded at 485 nm (*blue*) and 535 nm (*green*) from a single MIN6 cell by confocal microscopy. Note that the fluorescence signals moved in opposite directions: ECFP fluorescence increased and EYFP decreased after stimulation with exendin-4, reflecting a decrease in FRET. *C*, FRET donor/acceptor fluorescence emission ratio (*FL485/535*) measured in the cell from *A*. The increase in the ratio indicates an increase in $[cAMP]_c$. *D*, amplitude of the Epac1-camps response relative to the base line. Data are expressed as the FRET donor/acceptor fluorescence emission ratio at 485/535 nm normalized to the average base-line ratio values measured 1 min before stimulation (485/535 nm relative ratio). *E*, kinetics of cAMP production in a single MIN6 cell following application of forskolin (10 μM; *FSK*). Note that both exendin-4 and forskolin induced a monophasic increase in $[cAMP]_c$. Results are representative of ≥22 cells for each treatment.

measuring the effect of 2′,5′-dideoxyadenosine (DDA), a P-site inhibitor of membrane-bound AC isoforms. DDA inhibited cAMP formation stimulated by high K^+, tolbutamide, and glucose by 62, 63, and 66%, respectively (Fig. 2*D*).

Role of Calcium in cAMP Production in MIN6 Cells—Because it is well known that secretagogue stimulation increases $[Ca^{2+}]_c$, we next determined whether the cAMP responses are Ca^{2+}-dependent. The increases in $[cAMP]_c$ evoked by KCl (Fig. 3*A*), tolbutamide (Fig. 3*B*), and glucose (Fig. 3*C*) were abolished by removal of extracellular Ca^{2+} and by nitrendipine, a blocker of L-type voltage-dependent Ca^{2+} channels. Curve integration analysis indicated that cAMP production by high K^+, tolbutamide, and glucose was reduced by 114, 83, and 97%, respectively, when experiments were conducted in Ca^{2+}-free solutions (Fig. 3*E*). Ca^{2+} channel blockade with nitrendipine inhibited secretagogue-induced cAMP accumulation to similar levels (Fig. 3*E*). The contribution of intracellular Ca^{2+} store discharge to cAMP production was also assessed. Application of carbachol, a muscarinic agonist that stimulates inositol 1,4,5-trisphosphate formation and release of Ca^{2+} sequestered within the endoplasmic reticulum, in either the presence or absence of extracellular Ca^{2+} increased cAMP formation to levels ~10–20% of those caused by high K^+ or tolbutamide (Fig. 3, *D* and *E*). In some cells bathed in Ca^{2+}-free solutions, carbachol evoked a transient decrease in cAMP (17 of 48 cells), suggesting that transient release of Ca^{2+} from the endoplasmic reticulum activates phosphodiesterase (PDE) or inhibits AC. Reconstitution of extracellular Ca^{2+} following intracellular Ca^{2+} store depletion by carbachol stimulation in Ca^{2+}-free solutions increased cAMP production (data not shown), suggesting a role of Ca^{2+} entry through store-operated Ca^{2+} channels in mediating cAMP signaling in MIN6 cells. Our data indicate that secretagogue-induced elevation of cAMP con-

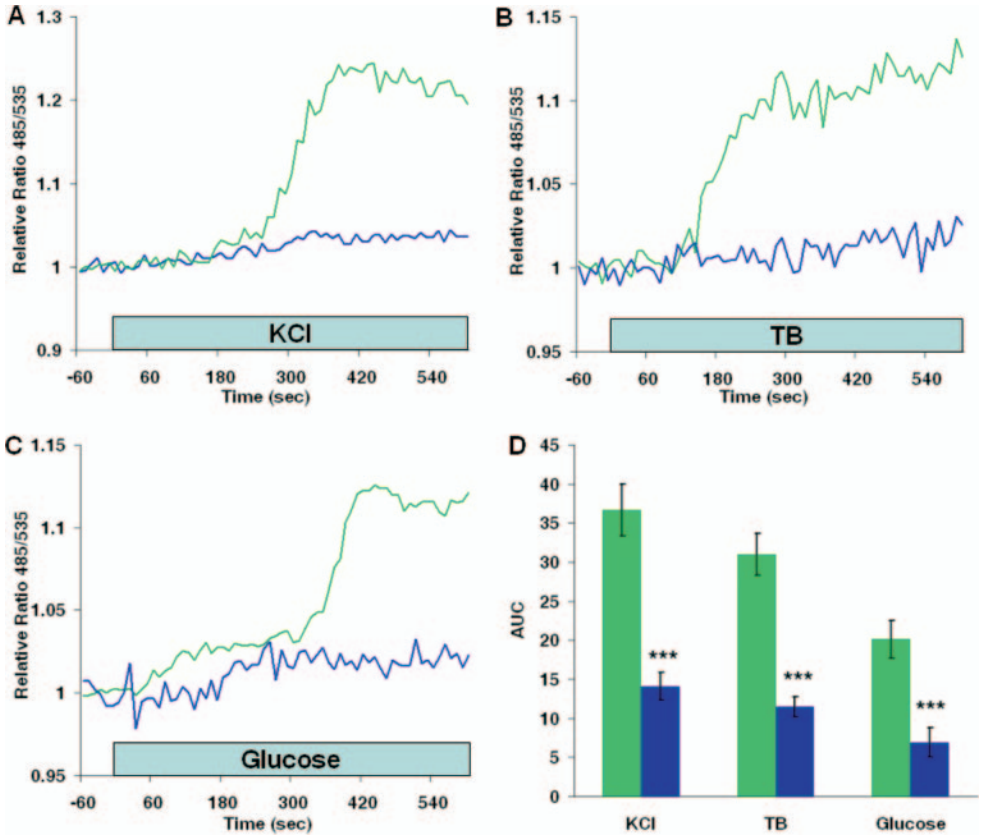

FIG. 2. **Effect of secretagogues on cAMP formation.** *A–C*, effects of 20 mM KCl, 100 μM tolbutamide (*TB*), and 20 mM glucose, respectively, on cAMP accumulation in the presence (*blue lines*) and absence (*green lines*) of 50 μM DDA, an inhibitor of membrane-bound adenylate cyclases. Cells were exposed to DDA 2–5 min prior to application of secretagogues. *D*, comparison of dynamic cAMP production following stimulation with secretagogues. Data are expressed as means ± S.E. ($n \geq 12$ cells) of the area under the 485/535 nm relative ratio curve (*AUC*) recorded during an 8-min (KCl or tolbutamide) or a 10-min (glucose) application of the stimulus (*green bars*). The effect of DDA (*blue bars*) and the statistical significance of comparisons with control responses for each stimulus are depicted. ***, $p < 0.001$.

centration is a Ca^{2+}-dependent signaling event requiring the influx of Ca^{2+} through voltage-gated Ca^{2+} channels and suggest that mobilization of endoplasmic reticulum Ca^{2+} stores plays a limited role in cAMP production.

Simultaneous Imaging of Cytoplasmic Calcium and cAMP—We determined the temporal interrelationships between cAMP and Ca^{2+} signaling by concurrent imaging of Epac1-camps FRET and Fura-2 dual wavelength ratiometric excitation microscopy. Fura-2 and Epac1-camps fluorescence was easily distinguished in MIN6 cells (Fig. 4*A*). In five independent experiments ($n = 24$ cells), stimulation with forskolin increased $[cAMP]_c$ and caused little or no change in $[Ca^{2+}]_c$ (Fig. 4*B*). The magnitude and temporal pattern of the forskolin-induced cAMP response in cells loaded with the Ca^{2+} indicator were similar to those observed in cells expressing only Epac1-camps (Fig. 1*E*), indicating that the presence of Fura-2 did not affect cAMP biosensor function or interfere with Ca^{2+}-dependent cAMP production.

Application of 20 mM KCl increased both $[Ca^{2+}]_c$ and $[cAMP]_c$. The Ca^{2+} response preceded cAMP accumulation in every cell we imaged ($n = 43$) (Fig. 4*C*). The amount of time before the initial rises in $[Ca^{2+}]_c$ and $[cAMP]_c$ was significantly different, occurring 47 ± 5 and 115 ± 9 s ($p < 0.001$), respectively, following addition of high K^+. Both signals rose to a new steady-state concentration and returned to base-line levels after K^+ was lowered. Similar monophasic responses were elicited by 100 μM tolbutamide (Fig. 4*D*), a sulfonylurea drug that increases $[Ca^{2+}]_c$ by activating β-cell Ca^{2+} influx through voltage-dependent Ca^{2+} channels consequent to closure of ATP-sensitive K^+ channels and membrane depolarization. The rise in $[cAMP]_c$ induced by tolbutamide lagged significantly behind the increase in $[Ca^{2+}]_c$ (59 ± 5 and 35 ± 5 s, respectively ($n = 15$ cells); $p < 0.001$). Glucose stimulation also increased $[cAMP]_c$; the delay between the Ca^{2+} and cAMP elevation was not statistically significant (264 ± 12 and 262 ± 14 s for $[cAMP]_c$ and $[Ca^{2+}]_c$, respectively ($n = 34$ cells); $p > 0.05$) (Fig. 4*E*).

Interplay between Intracellular Calcium and cAMP Oscillations—The data indicate a close temporal and causal interrelationship between increases in $[Ca^{2+}]_c$ and cAMP accumulation. This raises the possibility that Ca^{2+} oscillations elicit cAMP oscillations. In β-cells, stable and voltage-dependent Ca^{2+} oscillations with periodicities ranging between 0.5 and 10/min can be generated by glucose and other secretagogues. The combination of glucose stimulation in the presence of tetraethylammonium chloride (TEA), an inhibitor of K^+ channels, induces depolarization-dependent Ca^{2+} oscillations in rodent islets of Langerhans and insulin-secreting β-cell-like cell lines (23, 24). Application of 20 mM glucose and 20 mM TEA elicited rapid oscillations in $[Ca^{2+}]_c$ and $[cAMP]_c$ (Fig. 5*A*). The mean ± S.E. frequency of the coupled Ca^{2+} and cAMP oscillations was 0.50 ± 0.02/min (30.2 ± 1.2/h, $n = 32$ cells). Ca^{2+} oscillations were characterized by transient increases that returned to near base-line levels during the interspike phase. However, cAMP oscillations did not return to base-line levels. The transient spikes in $[Ca^{2+}]_c$ coincided with rapid decreases in $[cAMP]_c$ (Fig. 5*B*). During the quiescent period between Ca^{2+} oscillations, $[cAMP]_c$ gradually increased (Fig. 5*B*). To ascertain the role of extracellular Ca^{2+} in regulating $[cAMP]_c$ oscillations, we superfused the cells with Ca^{2+}-free solutions (Fig. 5*C*) or ap-

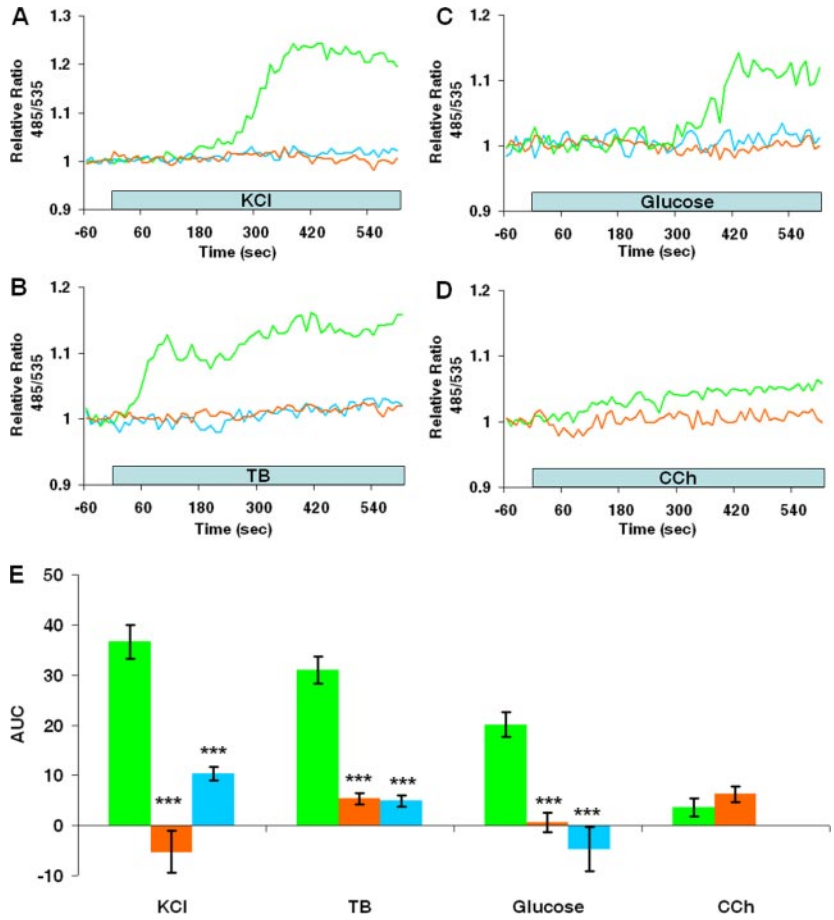

FIG. 3. **Ca^{2+}-dependent cAMP production in MIN6 cells.** *A–C*, effects of Ca^{2+}-free external solutions (0 added Ca^{2+} + 100 μM EGTA; *orange lines*) and nitrendipine (1 μM; *blue lines*) on cAMP production stimulated by 20 mM KCl, 100 μM tolbutamide (*TB*), and 20 mM glucose, respectively. Representative control responses conducted in parallel experiments are depicted (*green lines*). *D*, typical response of a MIN6 cell expressing Epac1-camps following application of 250 μM carbachol (*CCh*) in a Ca^{2+}-free superfusate (*orange line*). The traces shown in *A–D* are representative of results of three or more independent experiments. *E*, histogram of dynamic changes in the Epac1-camps 485/535 nm relative ratio. The results are means ± S.E. ($n \geq 12$ cells) of the area under the 485/535 nm relative ratio curve (*AUC*) during an 8-min (KCl, tolbutamide, or carbachol) or a 10-min (glucose) application of secretagogues under control conditions (*green bars*), in Ca^{2+}-free solutions (*orange bars*), and in the presence of 1 μM nitrendipine (*blue bars*). Statistical significance of comparisons with control responses is depicted. ***, $p < 0.001$.

plied nitrendipine (Fig. 5*D*), which caused rapid cessation of the Ca^{2+} oscillations and decreased $[Ca^{2+}]_c$. Under these conditions, cAMP oscillations were also ablated; however, unlike $[Ca^{2+}]_c$, $[cAMP]_c$ increased. These findings suggest Ca^{2+}-dependent activation of cAMP-hydrolyzing PDE by periodic and transient spikes of Ca^{2+} entry. We tested this hypothesis by administering 100 μM IBMX during the oscillations (Fig. 5*E*). As observed with low Ca^{2+} solutions, IBMX abolished cAMP oscillations and increased $[cAMP]_c$. DDA (50 μM) also inhibited cAMP oscillations, but did not increase $[cAMP]_c$ (Fig. 5*F*). Neither IBMX nor DDA inhibited Ca^{2+} oscillations. This indicates that the effects of these reagents on cAMP signaling did not stem from nonspecific effects on intracellular Ca^{2+}.

Expression of Adenylate Cyclase and Phosphodiesterase Isoforms in MIN6 Cells—To identify the AC and PDE isoforms involved in the regulation of Ca^{2+}-dependent cAMP signals in MIN6 β-cells, we used reverse transcription-PCR. We detected transcripts for Ca^{2+}-activated AC-I and AC-VIII isoforms as well as AC-IV–VII and AC-IX (see supplemental Fig. S1). A member of the Ca^{2+}-activated PDE1 family, PDE1C, was also expressed in MIN6 cells along with several other PDE isoforms, including PDE3A, PDE3B, PDE4A, PDE4B, PDE4C, PDE7B, and PDE10A (see supplemental Fig. S1).

DISCUSSION

The plasticity and diversity of cellular signals elicited by extracellular stimuli are determined by information encoded in specific patterns of spatial and temporal changes in Ca^{2+} and cAMP concentrations. Although it has long been suspected that these two major second messengers are dynamically integrated (1–3, 25), most studies have employed biochemical methods that lack sufficient temporal resolution necessary to simultaneously monitor cross-talk between cAMP and Ca^{2+} signal transduction cascades in single intact living cells. In this study, we combined a genetically encoded FRET-based cAMP biosensor approach and intracellular Ca^{2+} imaging with Fura-2 to determine the temporal and causal interrelationships between the cAMP and Ca^{2+} signaling pathways. Our data demonstrate a contribution of monophasic and oscillating Ca^{2+} signals to cAMP information encoding in electrically excitable insulin-secreting MIN6 β-cells.

Acute depolarization of MIN6 cells with high K^+, tolbutamide, or glucose caused a monophasic increase in cAMP. This agrees with other studies demonstrating that high K^+, applied either as a single-step increase or in pulsatile fashion, induces cAMP accumulation in PC12 cells and *Xenopus* neurons (17, 26). In MIN6 cells, the depolarization-induced accumulation of cAMP was significantly inhibited by DDA, suggesting that secretagogues stimulate membrane-bound AC activity. That Ca^{2+} plays a central role in stimulating AC was indicated by attenuation of cAMP formation following removal of extracellular Ca^{2+} or application of nitrendipine, an inhibitor of voltage-gated Ca^{2+} channels. This likely means that a Ca^{2+}-independent mechanism mediated by depolarization alone, voltage-dependent influx of Na^+, or K^+ conductance does not contribute to an increase in MIN6 cell cAMP, as has been proposed in *Paramecium*, *Lytechinus pictus* sperm, and neonatal rat cerebellar cells (27–29). Our observations in intact single cells confirm previous studies showing Ca^{2+}- and calmodulin-dependent activation of AC in murine islet lysates (30, 31).

The source of the Ca^{2+} signal was a critical determinant in establishing cross-talk between cAMP and Ca^{2+} second messenger systems; direct measurements of Ca^{2+} influx and cAMP in single intact MIN6 cells suggested that Ca^{2+} influx through

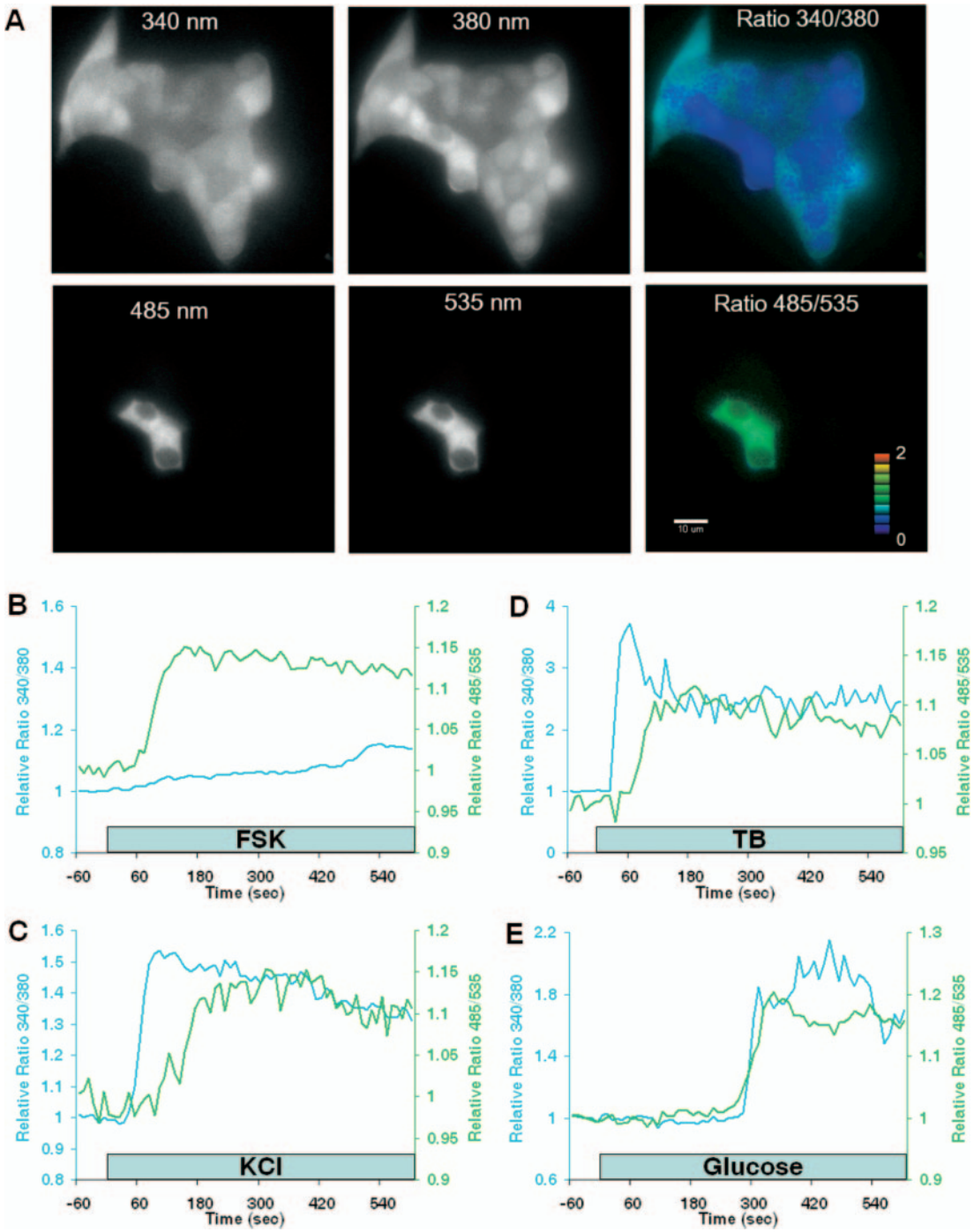

FIG. 4. **Simultaneous imaging of cytoplasmic Ca^{2+} and cAMP signaling.** *A*, 16-bit digital images of Fura-2-labeled MIN6 cells transiently expressing Epac1-camps. The image in each panel was recorded from the same field of view. Multiple excitation and emission optical filters were used to resolve Fura-2 (*340 nm* and *380 nm panels*) and Epac1-camps (*485 nm* and *535 nm panels*) fluorescence (see "Experimental Procedures" for details). The pseudo-colored displays of $[Ca^{2+}]_c$ (*Ratio 340/380 panel*) and $[cAMP]_c$ (*Ratio 485/535 panel*) show diffuse labeling of all cells with Fura-2 and only two cells expressing Epac1-camps. Note the spectral separation between the fluorescent indicators; it is easy to distinguish Epac1-camps expression in cells loaded with Fura-2. The *color bar* indicates the range of Epac1-camps FRET 485/535 nm ratio values depicted in the pseudo-colored display. *Scale bar* = 10 μm. *B*, effects of forskolin (*FSK*; 10 μM) on $[cAMP]_c$ (*green line*) and $[Ca^{2+}]_c$ (*blue line*) in a single MIN6 cell. The kinetics and amplitude of forskolin-induced cAMP production were not affected by Fura-2 loading. *C–E*, 20 mM KCl-, 100 μM tolbutamide (*TB*)-, and 20 mM glucose-induced gradients, respectively, of $[Ca^{2+}]_c$ and $[cAMP]_c$ in MIN6 cells. The traces are representative of cAMP and Ca^{2+} responses imaged simultaneously in individual cells (n $\geq$ 15 cells for each treatment).

nitrendipine-sensitive voltage-gated Ca^{2+} channels stimulated cAMP formation. This is in agreement with other studies that have shown partial inhibition of glucose- and glucagon-like peptide-1-stimulated cAMP accumulation in homogenates of rat primary β-cells by verapamil, a blocker of L-type Ca^{2+} channels (32). Entry of Ca^{2+} and other monovalent and divalent cations through L-type voltage-dependent and Ca^{2+} store-operated Ca^{2+} channels has been implicated in stimulating AC activity in rat C6-2B glioma cells and human embryonic kidney 293 cells transiently expressing Ca^{2+}-dependent AC-VIII (2, 33–35). On the other hand, evidence indicates that mobilization of intracellular Ca^{2+} stores does not activate AC in 1321N1 astrocytoma cells and A7r5 smooth muscle cells (36, 37). Rather than stimulate cAMP formation, discharge of endoplas-

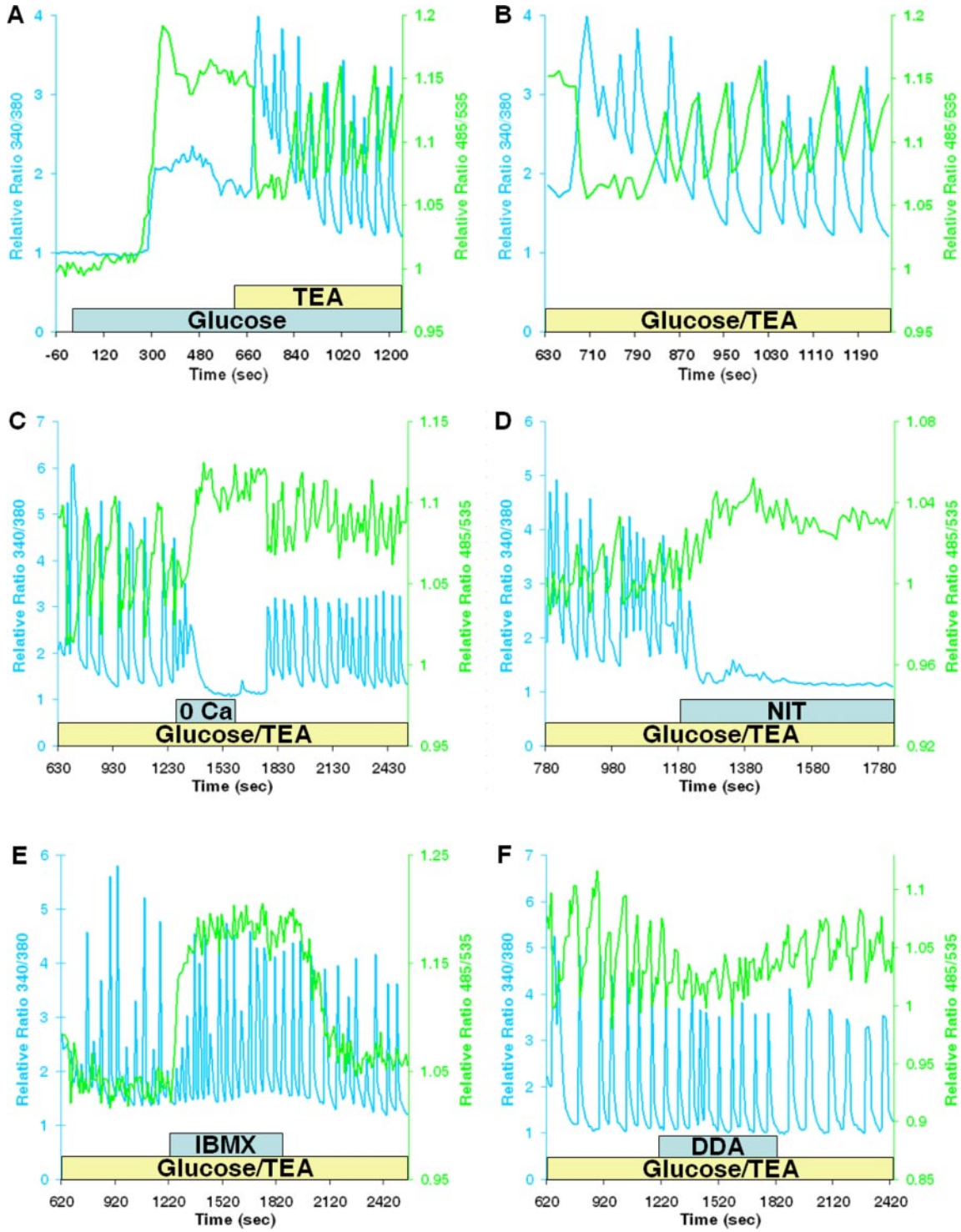

FIG. 5. **Intracellular Ca^{2+} and cAMP oscillations.** *A*, gradients of $[cAMP]_c$ (*green line*) and $[Ca^{2+}]_c$ (*blue line*) in a single MIN6 cell following application of 20 mM glucose and 20 mM TEA. Note the similar pattern of monophasic and multiphasic increases in Ca^{2+} and cAMP accumulation. *B*, detailed view of Ca^{2+} and cAMP oscillations generated by glucose and TEA in the cell depicted in *A*. The initial series of Ca^{2+} transients caused a rapid reduction in $[cAMP]_c$. cAMP oscillations occurred subsequent to the generation of additional transient spikes in Ca^{2+}. Second messenger oscillations were out of phase; note that each $[Ca^{2+}]_c$ spike was coupled to a rapid and transient reduction in $[cAMP]_c$. *C* and *D*, effect of removal of extracellular Ca^{2+} (*0 Ca*) or application of nitrendipine (*NIT*; 1 μM), respectively, during the second messenger oscillations stimulated by glucose and TEA. Superfusion with solutions containing Ca^{2+} restored the cAMP and Ca^{2+} oscillations. *E*, effect of 100 μM IBMX on cAMP and Ca^{2+} oscillations. *F*, cAMP and Ca^{2+} responses in a MIN6 cell stimulated with glucose and TEA in the presence of DDA (50 μM). Cells were continuously superfused with bicarbonate-buffered solutions at 37 °C.

mic reticulum Ca^{2+} induces a prolonged inhibition of AC (37). In electrically excitable A7r5 cells, phospholipase C-mediated Ca^{2+} release from intracellular sites of sequestration and activation of Ca^{2+}/calmodulin-dependent protein kinase II inhibit AC-III (37). This may represent an important negative feedback mechanism regulating cross-talk between Ca^{2+} and cAMP signaling. In this study, we found that application of carbachol and release of endoplasmic reticulum Ca^{2+} stores did not cause a marked increase in cAMP production in MIN6 cells. Whether carbachol or other agonists that mobilize intracellular

Ca^{2+} stores prevent cAMP rises consequent to MIN6 cell depolarization remains to be determined.

The concurrent measurements of $[cAMP]_c$ and $[Ca^{2+}]_c$ further support the hypothesis that cAMP formation is Ca^{2+}-dependent in MIN6 cells. Simultaneous imaging of both second messenger signals clearly showed that the rise in $[Ca^{2+}]_c$ stimulated by high K^+ and tolbutamide preceded cAMP accumulation. This is consistent with the increase in $[Ca^{2+}]_c$, subsequent to Ca^{2+} flux across the plasma membrane, driving production of cAMP and differs from observations in other cell types in which the elevation of $[cAMP]_c$ caused an increase in $[Ca^{2+}]_c$ (2, 3, 16). For example, in *R. esculenta* ventricular myocytes, simultaneous measurements of cAMP with FlCRhR and whole cell L-type Ca^{2+} current by patch-clamp electrophysiology revealed that cAMP responses precede Ca^{2+} currents following focal application of isoproterenol or forskolin. These findings raise the possibility that Ca^{2+} signaling depends on activation of AC and accumulation of cAMP (16). However, our results do not support this role of cAMP in MIN6 β-cells. Nevertheless, because our imaging studies were limited to measurements of global changes in second messenger signaling in single cells, the data do not rule out possible effects of focal or microdomain increases in cAMP on Ca^{2+} channel gating. We do not yet understand the molecular mechanisms underlying the delay between depolarization-induced increases in Ca^{2+} and cAMP. This may in part be explained by the amount of substrate (ATP) available for production of cAMP by AC. The glucose experiments support this possibility. Although glucose-induced cAMP accumulation was dependent on Ca^{2+} influx (Fig. 3*C*), unlike depolarization with high K^+ or tolbutamide, the Ca^{2+} and cAMP responses following glucose stimulation occurred concurrently. The most likely explanation is that glucose metabolism increases ATP production and augments the dynamic responses of Ca^{2+}-dependent production of cAMP. Additional studies will be necessary to explore this hypothesis.

Our findings provide compelling evidence directly linking oscillations in Ca^{2+} signaling with periodic cAMP accumulation by demonstrating, for the first time, simultaneous oscillations in $[Ca^{2+}]_c$ and $[cAMP]_c$ in single mammalian cells. The existence of cyclic nucleotide oscillations was originally suggested by pulsatile release of cAMP into the medium by *Dictyostelium* (38) and more recently shown to be coupled to spontaneous periodic changes in the mitogen-activated protein kinase ERK2 (extracellular signal-regulated kinase-2) (39). Coupling of cAMP oscillations to each contraction cycle in *Rana pipiens* cardiomyocytes has been proposed, but the temporal interrelationships between periodic cAMP changes and other signaling pathways were not evaluated (40). More recent studies using FRET measurements with FlCRhR have reported Ca^{2+}-dependent cAMP fluctuations in rat pheochromocytoma PC12 cells and *Xenopus* neurons (17, 26). Repetitive administration of high K^+ induces pulses of cAMP accumulation in *Xenopus* neurons that are dependent on extracellular Ca^{2+} (17). In our experiments, simultaneous imaging of Ca^{2+} and cAMP signaling revealed tightly coupled oscillations of $[cAMP]_c$ and $[Ca^{2+}]_c$ induced by endogenous oscillations in membrane potential and Ca^{2+} influx following glucose stimulation in the presence of TEA. Inhibiting Ca^{2+} influx by removal of extracellular Ca^{2+} or blockade of voltage-gated Ca^{2+} channels with nitrendipine ablated the cyclic nucleotide oscillations, confirming the essential role of Ca^{2+} influx in regulating cAMP oscillations.

We have not yet identified specific components of the cAMP signaling system involved in the generation of cAMP oscillations. AC and PDE, enzymes that regulate $[cAMP]_c$, have been proposed to mediate Ca^{2+}-dependent effects on cAMP signal transduction cascades (2–4). Diversity of cAMP signaling is determined by expression of multiple AC and PDE isoforms that are differentially regulated by Ca^{2+}, G-proteins, and protein kinases (6, 7, 41, 42). Individual cells express multiple AC and PDE isoforms that further contribute to signaling plasticity. Nine membrane-bound AC isoforms and a soluble AC isoform are expressed in mammalian cells (7). Inhibition of cAMP oscillations with DDA, a broad-spectrum inhibitor of membrane-bound AC, suggests a role of AC activity, but does not identify the specific isoforms involved or elucidate the role of soluble AC. Previous studies have shown that AC-I–VII and four splice variants of AC-VIII are expressed in islets and insulin-secreting cells (32, 43–45). Several AC isoforms are targets of Ca^{2+} signaling; AC-I and AC-VIII activity is stimulated by Ca^{2+}, whereas increased intracellular Ca^{2+} inhibits AC-III, AC-V, and AC-VI (7, 44, 46). Reverse transcription-PCR analysis revealed expression of AC-I and AC-VIII transcripts in MIN6 cells. This suggests that depolarization-induced Ca^{2+} influx causes cAMP formation by activation of AC-I or AC-VIII. Additional molecular studies are necessary to resolve the contribution of specific membrane-bound AC isoforms and to explore the role of soluble AC in Ca^{2+}-dependent cAMP accumulation following secretagogue stimulation.

The temporal interrelationships between Ca^{2+}-dependent AC and PDE activities that generate cAMP oscillations remain uncertain. Oscillations could be produced by periodic activation and deactivation of AC or PDE. Our data suggest, however, that the increase in $[Ca^{2+}]_c$ following secretagogue stimulation causes a sustained activation of AC. The temporal interrelationships between the $[Ca^{2+}]_c$ and $[cAMP]_c$ oscillations indicate that each transient increase in $[Ca^{2+}]_c$ is coupled to a rapid and transient decrease in $[cAMP]_c$ (Fig. 5, *A* and *B*). This effect is consistent with activation of Ca^{2+}-dependent PDE by the Ca^{2+} spikes. These observations suggest that periodic activation of PDE by the Ca^{2+} transients underlies the cAMP oscillations. This model is supported by our studies using IBMX, an inhibitor of PDE. IBMX blocked the cAMP oscillations and increased $[cAMP]_c$, but did not inhibit the Ca^{2+} transients. Reverse transcription-PCR analysis demonstrated expression of multiple PDE isoforms in MIN6 cells, including PDE1C, which is activated by calmodulin in a Ca^{2+}-dependent fashion (41, 47). Taken together, our findings suggest that dynamic interplay between Ca^{2+}-dependent AC-I and AC-VIII and PDE1C differentially encodes oscillatory Ca^{2+} signal inputs to generate cAMP oscillations in electrically excitable cells.

In summary, using newly developed biosynthetic FRET-based cAMP sensor technology in combination with a standard Ca^{2+} imaging approach, we have demonstrated, for the first time, Ca^{2+}-dependent amplitude and frequency encoding of cAMP signaling in MIN6 β-cells. Whether the results of our studies extend to other electrically excitable cells will be ascertained in future studies. Nonetheless, the temporal and causal interrelationships between cAMP and Ca^{2+} signaling suggest that the interplay between second messenger systems forms a signal transduction network capable of affecting and integrating multiple levels of signaling processes. This dynamic organization of second messenger signaling cascades may be essential in determining the specificity of cellular responses to extracellular stimuli.

Acknowledgments—We thank Drs. Louis H. Philipson, Matthew Brady, and Christopher Rhodes for helpful discussions and suggestions during the course of our studies.

REFERENCES

1. Rasmussen, H. (1981) *Calcium and cAMP as Synarchic Messengers*, Wiley InterScience, New York
2. Cooper, D. M. F., Mons, N., and Karpen, J. W. (1995) *Nature* **374,** 421–424
3. Zaccolo, M., and Pozzan, T. (2003) *Trends Neurosci.* **26** 53–55
4. Bruce, J. I. E., Straub, S. V., and Yule, D. I. (2003) *Cell Calcium* **34,** 431–444
5. Antoni, F. A. (1997) *Trends Endocrinol. Metab.* **8,** 7–14
6. Hurley, J. H. (1999) *J. Biol. Chem.* **274,** 7599–7602

7. Cooper, D. M. F. (2003) *Biochem. J.* **375,** 517–529
8. Ang, K.-L., and Antoni, F. A. (2002) *J. Neurochem.* **81,** 422–433
9. Maurice, D. H., Palmer, D., Tilley, D. G., Dunkerley, H. A., Netherton, S. J., Raymond, D. R., Elbatarny, H. S., and Jimmo, S. L. (2003) *Mol. Pharmacol.* **64,** 533–546
10. Nakade, S., Rhee, S. K., Hamanaka, H., and Mikoshiba, K. (1994) *J. Biol. Chem.* **269,** 6735–6742
11. Dean, W. L., Chen, D., Brandt, P. C., and Vanaman, T. C. (1997) *J. Biol. Chem.* **272,** 15113–15119
12. Holz, G. G., Leech, C. A., Heller, R. S., Castonguay, M., and Habener, J. F. (1999) *J. Biol. Chem.* **274,** 14147–14156
13. Kang, G., Chepurny, O. G., and Holz, G. G. (2001) *J. Physiol.* (*Lond.*) **536,** 375–385
14. Bruce, J. I., Yule, D. I., and Shuttleworth, T. J. (2002) *J. Biol. Chem.* **277,** 48172–48181
15. DeBernardi, M. A., and Brooker, G. (1996) *Proc. Natl. Acad. Sci. U. S. A.* **93,** 4577–4582
16. Goaillard, J.-M., Vincent, P., and Fischmeister, R. (2001) *J. Physiol.* (*Lond.*) **530,** 79–91
17. Gorbunova, Y. V., and Spitzer, N. C. (2002) *Nature* **418,** 93–96
18. Nikolaev, V. O., Bünemann, M., Hein, L., Hannawacker, A., and Lohse, M. J. (2004) *J. Biol. Chem.* **279,** 37215–37218
19. Grynkiewicz, G., Poenie, M., and Tsien, R. Y. (1985) *J. Biol. Chem.* **260,** 3440–3450
20. Palmer, A. E., Jin, C., Reed, J. C., and Tsien, R. Y. (2004) *Proc. Natl. Acad. Sci. U. S. A.* **101,** 17404–17409
21. Ponsioen, B., Zhao, J., Riedl, J., Zwartkruis, F., van der Krogt, G., Zaccolo, M., Moolenaar, W. H., Bos, J. L., and Jalink, K. (2004) *EMBO Rep.* **5,** 1176–1180
22. DiPilato, L. M., Cheng, X., and Zhang, J. (2004) *Proc. Natl. Acad. Sci. U. S. A.* **101,** 16513–16518
23. Roe, M. W., Worley, J. F., III, Mittal, A. A., Kuznetsov, A., DasGupta, S., Mertz, R. J., Witherspoon, S. M., III, Blair, N., Lancaster, M. E., McIntyre, M. S., Shehee, W. R., Dukes, I. D., and Philipson, L. H. (1996) *J. Biol. Chem.* **271,** 32241–32246
24. Roe, M. W., Worley, J. F., III, Qian, F., Tamarina, N., Mittal, A. A., Dralyuk, F., Blair, N. T., Mertz, R. J., Philipson, L. H., and Dukes, I. D. (1998) *J. Biol. Chem.* **273,** 10402–10410
25. Rapp, P. E., and Berridge, M. J. (1977) *J. Theor. Biol.* **66,** 497–525
26. Agnihotri, N., Kisaalita, W. S., and Keith, C. H. (1997) *J. Neurosci. Res.* **47,** 555–560
27. Schultz, J. E., Klumpp, S., Benz, R., Schurhoff-Goeters, W. J., and Schmid, A. (1992) *Science* **255,** 600–603
28. Beltran, C., Zapata, O., and Darszon, A. (1996) *Biochemistry* **35,** 7591–7598
29. Cooper, D. M. F., Schell, M. J., Thorn, P., and Irvine, R. F. (1998) *J. Biol. Chem.* **273,** 27703–27707
30. Karl, R. C., Zawalich, W. S., Ferrendelli, J. A., and Matschinsky, F. M. (1975) *J. Biol. Chem.* **250,** 4575–4579
31. Valverde, I., Vandermeers, A., Anjaneyulu, R., and Malaisse, W. J. (1979) *Science* **206,** 225–227
32. Delmeire, D., Flamez, D., Hinke, S. A., Cali, J. J., Pipeleers, D., and Schuit, F. (2003) *Diabetologia* **46,** 1383–1393
33. Chiono, M., Mahey, R., Tate, G., and Cooper, D. M. F. (1995) *J. Biol. Chem.* **270,** 1149–1155
34. Fagan, K. A., Mahey, R., and Cooper, D. M. F. (1996) *J. Biol. Chem.* **271,** 12438–12444
35. Fagan, K. A., Mons, N., and Cooper, D. M. F. (1996) *J. Biol. Chem.* **273,** 9297–9305
36. Goraya, T. A., Masada, N., Ciruela, A., and Cooper, D. M. F. (2004) *J. Biol. Chem.* **279,** 40494–40504
37. Dyer, J. L., Liu, Y., Pino de la Huerga, I., and Taylor, C. W. (2005) *J. Biol. Chem.* **280,** 8936–8944
38. Roos, W., Scheidegger, C., and Gerisch, G. (1977) *Nature* **266,** 259–261
39. Maeda, M., Lu, S., Shaulsky, G., Miyazaki, Y., Kuwayama, H., Tanaka, Y., Kuspa, A., and Loomis, W. F. (2004) *Science* **304,** 875–878
40. Booker, G. (1973) *Science* **182,** 933–934
41. Mehats, C., Andersen, C. B., Filopanti, S.-L., Jin, C., and Conti, M. (2002) *Trends Endocrinol. Metab.* **13,** 29–35
42. Houslay, M. D., and Milligan, G. (1997) *Trends Biochem. Sci.* **22,** 217–224
43. Leech, C. A., Castonguay, M. A., and Habener, J. F. (1999) *Biochem. Biophys. Res. Commun.* **254,** 703–706
44. Tian, Y., and Laychock, S. G. (2003) *Mol. Cell. Endocrinol.* **204,** 75–84
45. Guenifi, A., Portela-Gomes, G. M., Grimelius, L., Efendic, S., and Abdel-Halim, S. M. (2000) *Histochem. Cell Biol.* **113,** 81–89
46. Guillou, J.-L., Nakata, H., and Cooper, D. M. F. (1999) *J. Biol. Chem.* **274,** 35539–35545
47. Pyne, N. J., and Furman, B. L. (2003) *Diabetologia* **46,** 1179–1189